

Evolution of Packing Structure in Cyclic Mobility and Post-liquefaction of Granular Soils

Jiangtao Wei and Gang Wang

Abstract Micromechanical change in packing structures can provide significant insights to better understand the cyclic mobility and post-liquefaction behaviors of granular soils. In this study, Discrete Element Method (DEM) is used to investigate the evolution of the packing structure under undrained cyclic loading. The coordination number is used to indicate the formation and destruction of a load-carrying structure in the post-liquefaction stage. A new index, termed as centroid distance, is proposed to quantify the effect of void and particle redistribution during cyclic loading. The new index is found to have a strong correlation with the mobilized maximum cyclic strain in post-liquefaction deformation.

1 Introduction

Understanding the behaviors of cyclic mobility and liquefaction in granular soils has been a subject of intensive study for many decades (e.g., Seed and Lee 1966). Laboratory experiments have observed significant changes in soil behaviors before and after the initial liquefaction. For very loose sands, flow-type failure often occurs after the triggering of liquefaction. On the other hand, the mobilized strain in medium to dense sands continues to accumulate progressively in subsequent loading cycles, which is termed as “cyclic mobility” (Castro 1975). To date, there is no direct experimental observation regarding how the microscopic structure of the granular packing changes before and after the liquefaction. Researches on the post-liquefaction behaviors of granular soils are quite limited.

In this study, Discrete Element Method (DEM) is used to simulate the cyclic mobility and post-liquefaction behaviors of granular soils under undrained cyclic loading. The numerical investigation provides detailed microscopic information of

J. Wei · G. Wang (✉)

Department of Civil and Environmental Engineering,
The Hong Kong University of Science and Technology, Clear Water Bay,
Kowloon, Hong Kong
e-mail: gwang@ust.hk

the granular packing that cannot be obtained from conventional laboratory tests (e.g. Ng and Dobry 1994; Thornton 2000; Sitharam et al. 2009). Indexes will be proposed to quantitatively characterize the evolution of the granular packing structure. These indicators are found to have strong correlations with the cyclic mobility and post-liquefaction behaviors of the granular packing.

2 Discrete Element Simulation

In this study, an open source DEM code, Yade, is used to conduct the numerical simulations. 4,000 disk-shaped particles are randomly generated in a square representative volume element (RVE). Periodic boundary is prescribed on this RVE to eliminate the non-uniformity caused by RVE boundary. The radius of particles ranges from 0.15 to 0.45 mm and the mean radius $R_{50} = 0.3$ mm. A nonlinear Hertz-Mindlin model was used to describe the particle contact behavior. The following material properties are assigned to all the particles: Young's modulus of 70 GPa, Poisson's ratio of 0.3, friction coefficient of 0.5. After particles generation, the packing was isotropically consolidated under an initial confining pressure $p = 100$ kPa to reach a void ratio of 0.228.

The simulation was stress controlled quasi-static simple shear loading with constant volume prescribed and a cyclic stress ratio (CSR) of 0.2. The pore water pressure is determined by the difference of stress between the vertical total stress and the vertical effective stress. As shown in Fig. 1, the soil sample reached the initial liquefaction after 17 cycles. The simulated result is quantitatively similar to the laboratory test results of a dense granular sample, such as the gradual decrease of effective vertical stress in each load cycle till liquefaction, increase of shear strain with the number of load cycles, and phase transform from contraction to dilation in each load cycle. The double-amplitude maximum strain of each cycle before initial liquefaction increases slowly to 2.1 % at cycle No. 17 when the initial liquefaction occurs. From cycle No. 17 to 22, the maximum strains increase dramatically. After cycle No. 22, the mobilized maximum strain is saturated to around an ultimate value, which will be further discussed later.

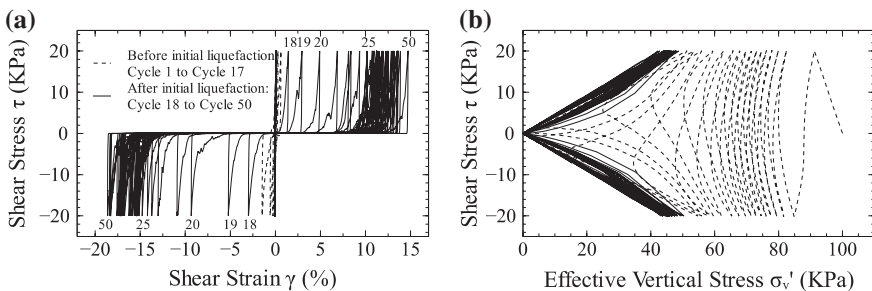


Fig. 1 Macroscopic behaviors of granular packing from DEM. **a** Shear stress and shear strain relation. **b** Shear stress and effective vertical stress relation

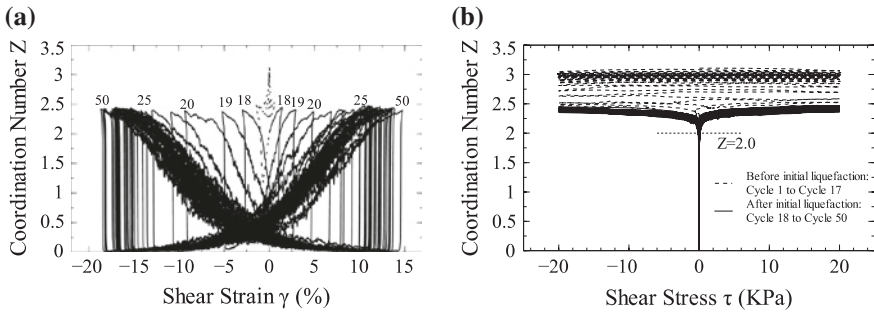


Fig. 2 **a** Coordination number and shear strain relation. **b** Relation between coordination number and shear stress

3 Micromechanical Structure During Post-liquefaction Stage

3.1 Evolution of the Coordination Number

The coordination number is a good indicator of the micromechanical load-carrying structure since it represents the average number of contacts for each particle, which is defined as $Z = 2N_c/N_p$ (where N_c is the total number of contacts and N_p is the total number of particles). Figure 2 shows the evolution of Z during the cyclic loading process. Initially, the coordination number is 3.1, and the material behaves almost elastically. The contact number decreases in each subsequent loading cycle. During post-liquefaction, the circulate loop like butterfly wings in Fig. 2a.

Liquefied sand experiences a large flow-type deformation and eventually regains strength under continued shear deformation, which is regarded as shear-induced dilatancy, i.e., the tendency of the granular matter to dilate under shear deformation. Figure 3 shows the stress-strain relationship and evolution of the coordination number versus the shear stress during cycle No. 19 (post-liquefaction). The shear stress remains almost zero at point 0 and starts to increase when the shear strain $\gamma = 1.13\%$ at point 1, where the shear stress reaches 0.1 kPa. This stage is termed as the “flow stage”. The flow stage is followed by a “hardening stage” when the shear stress starts to grow substantially to 20 kPa. The coordination number reaches 2.39 from point 1 to 2. Comparing with the peak stress point 2, there are 84 % of the contacts established at the end of the flow stage (i.e. point 1). These contacts form a load-carrying structure that permits stress to increase during further shear deformation. Figure 2b clearly demonstrates a threshold contact number ($Z = 2$) needed for establishment of such a loading-carry structure. Another interesting phenomenon observed from the Fig. 3 is that immediately upon unloading (from point 2 to 3), the coordination number decreases dramatically to reach a minimum value ($Z = 0.1$), implying that the load-carrying structure is completely destroyed upon stress reversal.

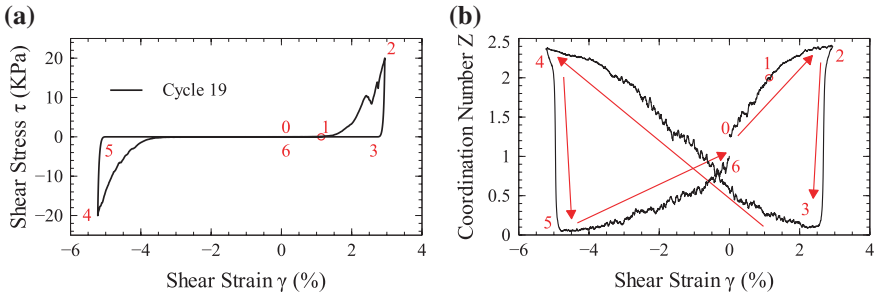


Fig. 3 Stress-strain relation and evolution of coordination number during cycle number 19 (a, b)

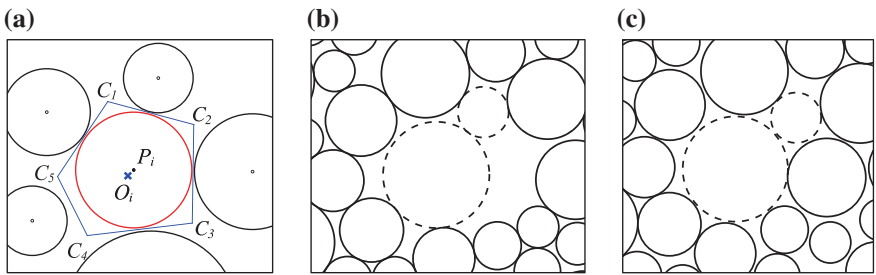


Fig. 4 a Definition of D_c^i . b Packing configuration before cyclic loading. c Packing configuration after 50th loading cycle

3.2 Definition of Centroid Distance (D_c)

For 2D DEM simulation, Voronoi cell can be conveniently used to divide the void space around each particle. As shown in Fig. 4a, the Voronoi cell for particle i is a convex polygon enclosed by C_1 – C_2 – C_3 – C_4 – C_5 . The mass center of the Voronoi cell and the mass center of the particle are denoted as O_i^i and P_i^i , respectively. The centroid distance for particle i can be defined as $D_c^i = |P_i^i - O_i^i| / R_{50}$, where R_{50} is the average radius of particles in the packing. Snapshots of particle configuration before cyclic loading (under effective confining stress of 100 kPa) and after 50 loading cycle (effective stress is almost zero) are illustrated in Fig. 4b, c. A relatively large pore is surrounded by particles in dotted line in the initial configuration. After cyclic loading, the large pore diminishes, and D_c^i of the particles in dotted line decreases considerably. The above observation corroborates the suggestion by Youd (1977), who attributed the pore-pressure buildup in saturated soils to collapse of unstable particles within the packing. The centroid distance appears to be an effective indicator to quantify the pore space redistribution in undrained cyclic loading.

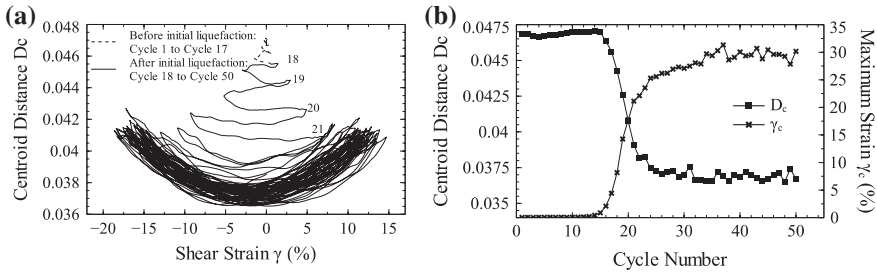


Fig. 5 Simulated results for stress-controlled test with CSR = 0.2: **a** D_c versus shear strain, **b** evolution of γ_c and D_c with the number of cycles

3.3 Evolution of D_c and Cyclic Mobility in Post-liquefaction

The centroid distance (D_c) of the whole packing can be defined as the average of D_c^i over all particles: $D_c = (\sum_i^N D_c^i)/N$, where N is the number of particles. Through the DEM simulation, it is observed that the cyclic mobility of the granular packing is strongly correlated to the evolution of D_c .

Figure 5a shows the evolution of D_c with the shear strain γ during 50 loading cycles. In the first 25 cycles, D_c decreases almost monotonically. In the following load cycles, D_c increases during loading and then decreases upon unloading, with a net effect of decrease in value after a full loading cycle. After approximately 30 loading cycles, D_c reaches a lower-bound limit.

Here, we use γ_c to measure the maximum mobilized (double-amplitude) strain in each load cycle. For example, γ_c is calculated as the shear strain between point 2 and 4 in Fig. 3a for load cycle No. 19. The relation between γ_c and D_c is illustrated in Fig. 5b, where D_c in the figure refers to its minimum value within a loading cycle. Interestingly, significant change in D_c and γ_c occurs simultaneously from cycle No. 17 (the initial liquefaction) to cycle No. 22. When D_c reaches its lower limit, the mobilized maximum shear strain γ_c also stabilizes around a constant value. The maximum shear strain ceases to increase under further loading cycles, and the stress–strain behavior of the soil is eventually saturated.

The evolution of D_c indicates change in granular packing in cyclic loading. Due to the friction between granular particles and complex particle shape, a local arching structure can be formed during initial consolidation, which preserves relative large pores. More large pores can be observed in the loose packing compared with the dense or medium dense packing under the same stress condition. However, the arching structure is not stable and can be progressively destroyed during the cyclic loading. As large pores are redistributed during cyclic loading, the packing is more homogeneous and D_c decreases accordingly.

4 Conclusions

In this study, DEM is used to simulate the cyclic mobility and post-liquefaction behaviors of granular soil under undrained cyclic loading. The coordination number is used to quantify the change in the load-carrying structure of the granular packing. Upon initial liquefaction, the coordination number significantly reduces to almost zero when particles lose contact, and it gradually increases when the packing continues to deform. A load-carrying structure can be gradually formed in the post-liquefaction stage to sustain considerable load when the coordination number exceeds a threshold value. The granular packing exhibits dilative behavior and strain hardening. However, the load-carrying structure can be completely destroyed upon stress reversal, as indicated by the immediate reduction of the coordination number to near zero. To quantify the change in microscopic configuration during cyclic loading, centroid distance is defined as an effective indicator to quantify the physical process of pore and particle redistribution. It is found that the centroid distance of the packing is strongly correlated to the cyclic mobility in the post-liquefaction stage. The numerical simulation reveals the existence of an ultimate stage for the centroid distance of the packing, and correspondingly, saturation of the maximum shear strain that can be mobilized in post-liquefaction deformation.

Acknowledgments The study was financially supported by Research Project Competition (UGC/HKUST) grant No. RPC11EG27 and DAG11EG03G.

References

- Castro G (1975) Liquefaction and cyclic mobility of saturated sands. *J Geotech Eng Div ASCE* 101(GT6):551–569
- Ng TT, Dobry N (1994) Numerical simulations of monotonic and cyclic loading of granular soil. *Int J Geotech Eng* 120(2):388–403
- Seed HB, Lee KL (1966) Liquefaction of saturated sands during cyclic loading. *J Soil Mech Found Eng ASCE* 92:105–134
- Sitharam TG, Vinod JS, Ravishankar BV (2009) Post-liquefaction undrained monotonic behavior of sands: experiments and DEM simulations. *Géotechnique* 59(9):739–749
- Thornton C (2000) Numerical simulations of deviatoric shear deformation of granular media. *Géotechnique* 50(1):43–53
- Youd TL (1977) Packing changes and liquefaction susceptibility. *J Geotech Eng Div ASCE* 103(8):918–922